Age-associated B cells are critical for the control of latent gammaherpesvirus 68 infection

Isobel C. Mouat[1], Iryna Shanina[1], Marc S. Horwitz[1]

[1] Department of Microbiology and Immunology, The University of British Columbia, Vancouver, British Columbia, Canada

Corresponding author:
Marc S. Horwitz
Room 3551, Life Sciences Centre
2350 Health Sciences Mall
University of British Columbia
Vancouver, B. C. Canada V6T 1Z3
604-822-6298
mhorwitz@mail.ubc.ca

Abstract

Age-associated B cells (ABCs; CD19^{+}CD11c^{+}T-bet^{+}) are increased during an array of viral infections, though their role during viral latency is unexplored. Here, we use murine gammaherpesvirus 68 (γHV68), a homolog of Epstein-Barr virus that latently infects B cells, to demonstrate that ABCs are necessary for the effective control of gamma-herpesvirus latency. We observe that ABCs expand in the spleen during acute infection and persist at least 150 days post-infection. During acute and latent infection ABCs secrete IFNγ and TNF. Using a strain of γHV68 that is cleared following acute infection, we show that ABCs persist in the absence of latent virus, though they secrete less IFNγ and TNF. With a fluorescent virus we demonstrate that ABCs are infected with γHV68 at similar rates to other mature B cells. We find that mice without ABCs display defects in anti-viral IgG2a/c antibodies and are less able to maintain γHV68 latency when challenged with heterologous infection. Together, these results indicate that ABCs are a persistent subset during latent viral infection that controls γHV68 reactivation from latency.

Conflict of interest statement

The authors have declared that no conflict of interest exists.

Introduction

Humans are infected with an array of herpesviruses that persist within us throughout our lives and require continuous surveillance by the host immune system. Gammaherpesvirus-68 (γHV68), like other herpesviruses, deploys distinct transcriptional programs during lytic and latent infection, each of which requires a distinct immune response, though the immunological requirements to maintain latency are incompletely understood[1]. Age-associated B cells (ABCs) are a recently identified unique B cell population implicated in viral infection, autoimmunity, and aging[2–4]. ABCs ($CD19^{+}CD11c^{+}T\text{-}bet^{+}$) are induced following γHV68 infection[5], though their function throughout infection is not clear. In this study we examine the response of and role for ABCs throughout γHV68 infection, from acute infection through long-term latency.

ABCs were identified in 2011 in the context of female aging and autoimmunity[2,3] and have since been shown to be increased in an array of viral infections including lymphocytic choriomeningitis virus (LCMV), murine cytomegalovirus, γHV68, vaccinia, human immunodeficiency virus, rhinovirus, SARS-CoV2, and influenza[5–10]. ABCs are elevated in the spleen and circulation during active viral infections and persist primarily in the spleen during chronic infection or upon infection resolution[7,8]. ABCs display multiple functional capacities including the secretion of antibodies and anti-viral cytokines, and activation of T cells[11,12]. T-bet expression in B cells is required for IgG2a/c class switching[13] and lack of ABCs exacerbates LCMV chronic infection in mice[14]. We predict that ABCs could be playing a role throughout γHV68 infection due to their long-term persistence, activation of T cells, and continuous cytokine and antibody production.

Lytic γHV68 infection is primarily cleared by $CD8^+$ T cells[15,16], following which γHV68 persists in a latent state mainly in quiescent mature B cells[17]. During latency the immune response persists even though there is minimal production of viral genes and limited production of new virions[18]. Both humoral and cellular responses contribute to controlling γHV68 infection long-term(3–8)[19,20]. Mice lacking either antibodies or T cells are both able to control γHV68 latency, though mice lacking both antibodies and T cells display elevated γHV68 reactivation[19,21]. IFNγ is critical for controlling γHV68 replication and reactivation from latency[22,23]. B cells are also known to be important during latent γHV68 infection. B cells act as the primary latent viral reservoir, B cells are required for movement from the lung to the spleen at the onset of latency, and mice deficient in B cells are unable to develop latency[17,24–26]. B cells secrete anti-viral antibodies long term[27], but also may contribute to the maintenance of latency through the secretion of anti-viral cytokines or help to virus-specific T cells. The precise B cell subsets, mechanisms, and factors that facilitate the control of viral latency and prevent reactivation are not fully understood.

The role of ABCs during acute and latent herpesvirus infection is unknown. Herein, we use γHV68 to investigate the role of ABCs throughout lytic and latent gammaherpesvirus infection. Using various tools, we investigate the relationship between γHV68 and ABCs throughout infection. We find that ABCs expand during acute γHV68 infection and persist during latency and that ABCs continuously respond to the latent virus by secreting anti-viral cytokines. In the

face of heterologous challenge, ABCs are required for controlling reactivation from latency. Thus, our findings highlight a novel role for ABCs in preventing gammaherpesvirus reactivation.

Results

ABCs are induced and maintained following γHV68 infection in a sex-biased manner

To examine the relative proportion of ABCs during acute and latent γHV68 infection, C57BL/6(J) mice were mock-infected with media (naïve) or infected with γHV68 for 6, 35, and 150 days, blood and spleen were collected and analyzed by flow cytometry to measure ABCs using a gating scheme described in Figure 1A that identified CD11c^{+}T-bet^{+} as a proportion of mature B cells (CD19^{+}IgD^{-}). We observed the relative proportion of ABCs increased in circulation during acute γHV68 infection (6 days p.i.) compared to naïve mice (Figure 1B-C). The proportion of circulating ABCs then decreased to pre-infection levels during latent γHV68 infection (35 and 150 days p.i., Figure 1B-C). This indicates that ABCs circulate in response to the lytic γHV68 infection but do not remain elevated in circulation during latency. In the spleen, the relative proportion and total number of ABCs was increased during acute γHV68 infection (day 6 p.i.) relative to naïve mice and remained elevated during latent γHV68 infection at 35 days p.i. and 150 days p.i. (Figure 1D-E, Figure S1). These results support previous findings that the spleen is the major site for ABCs during acute infection[8].

Intriguingly, we observed that the proportion of ABCs is increased in females as compared to males in both the blood and spleen throughout infection (Figure 1F-M). Previously, we

demonstrated that ABCs display a sex bias during experimental autoimmune encephalomyelitis and at 35 days post-γHV68 infection in the spleen[28]. Here, we have extended this finding and shown that ABCs display female sex bias in both the circulation and spleen during lytic and latent γHV68 infection. While ABCs increase in both females and males following γHV68 infection, there is a sex bias leading to greater expansion in females. These results demonstrate that ABCs are increased in circulation during acute γHV68 infection and continue to endure in the spleen long-term during latent infection.

ABCs express anti-viral cytokines in response to latent γHV68 infection

To begin investigating the role of ABCs in the anti-viral response, we measured ABC expression of anti-viral cytokines interferon-γ (IFNγ) and tumor necrosis factor-α (TNF) in the spleen at 6, 35, and 150 days p.i.. We found that during acute γHV68 infection (6 days p.i.), roughly 40% of ABCs in the spleen expressed IFNγ and TNF, as compared to about 10% of ABCs in naïve mice (Figure 2A-B). During latent infection (35 days and 150 days p.i.), a significantly increased proportion of ABCs continued to express IFNγ and TNF compared to naïve mice, though the proportion of ABCs expressing IFNγ and TNF was decreased compared to acute infection (Figure 2A-B). Throughout the acute and latent infection, we observed a downregulation of IL-17A expression on ABCs (Figure 2C).

To determine if the level of cytokine expression was distinct from other B cells, we compared the proportion of ABCs expressing IFNγ and TNF to non-ABC B cells. Specifically, we examined expression on ABCs compared to $CD11c^{-}Tbet^{+}$ and $CD11c^{-}Tbet^{-}$ B cells 35 days post-γHV68

infection (Figure 2D). We found that a significantly increased proportion of ABCs express IFNγ and TNF than non-ABC B cells, both CD11c$^-$Tbet$^+$ and CD11c$^-$Tbet$^-$ B cells, in the spleen (Figure 2E). The mean fluorescent intensity (MFI) of IFNγ and TNF, of IFNγ or TNF positive cells, was significantly increased on ABCs compared to both non-ABC populations (Figure S2A, B). CD11c$^-$Tbet$^+$ B cells expressed an intermediate level of IFNγ and TNF between ABCs and CD11c$^-$Tbet$^-$ B cells (Figure 2E, Figure S2A, B). Further, we examined the expression of IL-17A on ABCs and found reduced levels at all time points when compared to naïve mice. Additionally, sex differences in cytokine expression were not observed (Figure 2A-C, Figure S3 A-C). As more than 20% of ABCs continued expressing IFNγ and TNF during latency, and that ABCs still expressed significantly more IFNγ and TNF than any other B cell subset, indicates that ABCs are likely functioning in a unique anti-viral capacity during latent infection.

To explore the relationship between latent γHV68 and the ABC population, we infected mice with ACRTA-γHV68, a recombinant strain of γHV68 in which the genes responsible for latency are deleted and a lytic gene, RTA, is constitutively expressed[29]. As a result, γHV68 infection is cleared following acute infection without ever establishing latency. We found that, at 35 days p.i., a time point at which ACRTA-γHV68 is cleared, ABCs are increased to the same level in the spleens of ACRTA-γHV68 infected mice as compared to spleens in mice infected with WT γHV68 (Figure 2F). Thus, ABCs persist in the absence of latent virus, indicating that ABCs act similar to memory cells that remain following acute infection. However, we observed that the proportion of ABCs in ACRTA-γHV68-infected mice expressing IFNγ and TNF at 35 days p.i. was significantly reduced compared to those infected with WT γHV68 while remaining significantly elevated

compared to naïve mice (Figure 2G-H). Additionally, the IFNγ^{+} ABCs in mice infected with ACRTA-γHV68 displayed a lower MFI than those from γHV68-infected mice, though the TNF MFI was not significantly different between the two groups (Figure S2C, D). Without the presence of the latent virus, we observe a decrease specifically in the proportion of ABCs that doubly express IFNγ and TNF (Figure 2I). This finding indicates that ABCs respond to the latent virus by producing both IFNγ and TNF.

Together, these results show that ABCs are the predominant B cell subset expressing anti-viral cytokines IFNγ and TNF during acute and latent γHV68. Further, our data establish that high levels of expression of these cytokines was dependent on the presence of the virus. These findings suggest that ABCs recognize the presence of the quiescent latent virus and respond by expressing anti-viral cytokines, raising the possibility that ABCs play an important role in controlling latent virus.

ABCs are susceptible to γHV68 infection but are not a major viral reservoir

γHV68 is known to infect B cells, in particular mature or memory B cells[30–33]. To determine if ABCs are directly infected by γHV68, we used a previously developed fluorescent strain of γHV68, γHV68.H2bYFP[34]. Mice were infected with γHV68.H2bYFP and 8 days p.i. spleens were collected, and flow cytometry was performed. When we attempted to examine a later time point (16 days p.i.), we were unable to detect fluorescence. We found that during acute infection, a small proportion of ABCs were infected with γHV68. The same proportion of ABCs were positive for the fluorescent virus (1.2 ± 0.3%) as observed in mature B cells (1.1 ± 0.2%,

Figure 3A-B), demonstrating that ABCs are not preferably targeted for infection. To our knowledge this is the first evidence of a virus directly infecting ABCs. We next asked what proportion of the γHV68 reservoir is made up of ABCs. The primary reservoir for γHV68 is mature B cells which aligns with our results that 66% of γHV68-infected cells are mature B cells (Figure 3C). We found that ABCs make up only 5% of γHV68-infected cells (Figure 3C). Other infected cell populations included innate cells such as macrophages, DCs, and NK cells, as well as a small proportion of T cells (Figure 3C). We also examined the relationship between infection of ABCs and expression of IFNγ. We observed that during acute infection the proportion of ABCs expressing IFNγ was significantly lower in ABCs infected with γHV68 (4.3±1.3 %) as compared to uninfected ABCs (32.2±1.0%, Figure 3D). These results indicate that direct infection of ABCs was not driving IFNγ production and that during acute infection ABCs are susceptible to γHV68-driven downregulation of IFNγ. These findings demonstrate that although a portion of ABCs are infected with γHV68, ABCs are not the major target for γHV68.

ABCs are dispensable for the control of acute infection and establishment of latency

To further examine the role(s) of ABCs in γHV68 infection, mice with a floxed B cell specific T-bet deletion were followed post-infection. Specifically, *Tbx21*$^{fl/fl}$*Cd19*$^{cre/+}$ (KO) and littermate *Tbx21*$^{fl/fl}$*Cd19*$^{+/+}$ (Ctrl) mice were infected with γHV68 for 6 or 35 days and the spleen was collected to examine lytic and latent infection by qPCR and the immune cell composition (Figure 4A). Mice were genotyped by PCR and loss of ABCs in KO mice was confirmed by flow cytometry (Figure 4A). No differences in clinical symptoms or weight changes were observed during γHV68 infection between Ctrl or KO mice (Figure S4A).

To determine if knocking out ABCs alters immune cell composition, Ctrl and KO mice were infected or mock-infected with γHV68 and spleens analyzed at 6 or 35 days by flow cytometry to examine various T cell, B cell, and innate immune cell populations. No difference in the total number of splenocytes was observed (Figure S4B). The composition of the splenic immune profile was similar between Ctrl and KO mice with no significant differences observed in the relative proportions of B cells, CD8 T cells, DCs, neutrophils, NK cells, or macrophages between mock-infected mice or those infected with γHV68 for 6 or 35 days, though KO mice had greater proportions of CD4 T cells than Ctrl mice 35 days post-infection (Figure S5).

To examine the role of ABCs in controlling γHV68 infection we first measured viral load by qPCR in the spleens of Ctrl and KO mice infected with γHV68 for 6 and 35 days. We found no difference in that the quantity of γHV68 at 6 and 35 days p.i. between Ctrl and KO mice (Figure

4C-D). As expected, the quantity of γHV68 did not differ between male and female mice (Figure S6). To confirm that KO mice effectively control the lytic infection and develop latency, we infected Ctrl and KO mice with latency-deficient ACRTA-γHV68 for 35 days. We found that KO mice, like Ctrl mice, displayed similar viral loads that were near or below the limit of detection when infected with ACRTA-γHV68 (Figure 4E). As no virus was detected at day 35, mice lacking ABCs were effectively controlling the lytic infection. Furthermore, no differences were observed in the relative expression of viral genes associated with lytic infection (*Orf50*, *Orf68*) or latent infection (*Orf73*) between Ctrl and KO mice (Figure 4F). *Orf50* encodes the replication and transcription activator protein, which initiates viral lytic gene expression[35]. *Orf68* encodes a packaging protein that assists in moving the newly replicated viral genomes to the packaging motor, where they are loaded into capsids[36]. *Orf73* encodes for the latency-associated nuclear antigen that is required for the establishment and maintenance of latent infection[37,38]. As such, equal expression of lytic and latency-associated genes *Orf50*, *Orf68,* and *Orf73* between Ctrl and KO mice strongly suggests that Ctrl and KO mice harbor similar levels of lytic and latent γHV68. Together, these results demonstrate that ABCs are not required for the clearance of acute infection and establishment of latency in steady-state conditions.

Lack of ABCs results in a dysregulated γHV68 antibody response but does not alter the viral reservoir or anti-viral T cell response

ABCs are known to secrete anti-viral IgG2a/c[5], and transfer of serum into mice without ABCs during LCMV infection was partially able to restore control of the infection[14]. To examine the antibody response in Ctrl versus KO mice, mice were infected with γHV68 for 35 days and sera

226 was collected. The levels of anti-γHV68 IgG were the identical between Ctrl and KO mice,
227 though Th1-associated IgG2c was significantly decreased in KO mice, while Th2-associated IgG1
228 was significantly elevated when compared to Ctrl mice (Figure 5A-C). These results suggest that
229 ABCs are the primary secreters of anti-γHV68 IgG2, though in their absence there is
230 compensation by other B cell subsets resulting in increased anti-γHV68 IgG1 antibodies.
231
232 We next asked if the γHV68 reservoir was altered in mice without ABCs, as a portion of γHV68-
233 infected cells were ABCs. In particular, we posited that an altered viral reservoir could impact
234 the ability of KO mice to maintain γHV68 latency; previous findings indicate that various cell
235 types infected by γHV68 may display differential susceptibility to reactivation[22,39]. To compare
236 the viral reservoir in Ctrl and KO mice, we infected mice with a fluorescent strain,
237 γHV68.H2bYFP, and, at 8 days p.i., examined immune cell populations that comprise the γHV68-
238 infected population. We observed no difference in the proportion of infected cell populations,
239 including T cells, DCs, macrophages, NK cells, and immature and mature B cells (Figure 5D). This
240 suggests that the cell populations infected with γHV68 are not substantially altered in KO mice
241 compared to Ctrl mice, making it unlikely that changes to the reservoir impacted susceptibility
242 to viral reactivation.
243
244 To ask whether ABCs influence anti-viral immune cells in the spleen. We examined three cell
245 populations previously shown to be important for control of latent γHV68: IFNγ-producing cells,
246 γHV68-specific $CD8^+$ T cells, and $V\beta4^+CD8^+$ T cells. IFNγ is present at low levels during latency[40]
247 and is critical for controlling γHV68 reactivation from latency[22,23,41]. In particular, IFNγ-

248 producing T cells are known to block γHV68 reactivation[22,42–44]. $CD8^+$ T cells that harbor the Vβ4
249 TCR were also examined. $CD8^+V\beta4^+$ T cells expand following γHV68 infection and reach their
250 highest levels during latency, wherein they persist throughout infection without taking on an
251 exhausted phenotype[45–47]. γHV68-specific $CD8^+$ T cells were also measured with tetramers to
252 p79, an immunodominant γHV68 epitope for which CD8-specific memory T cells remain
253 throughout latent infection[48]. We observed that the proportion of $CD4^+$ and $CD8^+$ T cells that
254 express IFNγ were unchanged between mice with and without ABCs (Figure 5E-F). Further, no
255 differences were observed in the proportion of either $V\beta4^+CD8^+$ T cells or γHV68 p79-specific
256 $CD8^+$ T cells between mice with and without ABC circulating populations (Figure 5G-H).
257 Additionally, we found that the proportion of NK cells and B cells that express IFNγ, and the MFI
258 of IFNγ on these populations, was not changed between Ctrl and KO mice whether mock-
259 infected or infected for 6 or 35 days (Figure S7). That a similar proportion of B cells expressed
260 IFNγ indicates that another B cell subset likely compensates for the loss of IFNγ-expressing
261 ABCs. Collectively, these findings indicate that ABCs are not acting to stimulate anti-viral
262 immune cell populations in the spleen.
263
264 Together, these data indicate that knocking out ABCs leads to dysregulation of the γHV68
265 antibody response, without altering the γHV68 reservoir or T cell populations responding to the
266 latent virus.
267

268 Susceptibility to γHV68 reactivation increases in the absence of ABCs

269 We posited that the persistence of ABCs long-term during γHV68 and their secretion of IFNγ,

270 TNF, and anti-viral antibodies suggest that ABCs have an important role in the maintenance of
271 latency and suppression of γHV68 reactivation. To examine this role, ex vivo reactivation assays
272 were performed on splenocytes from Ctrl and KO mice at 35 days p.i.. Splenocytes from γHV68-
273 infected KO mice reactivated more frequently in culture than those from Ctrl mice, indicating
274 an increased propensity for γHV68 reactivation in the absence of ABCs (Figure 6A). This assay
275 does not disentangle whether infected cells have an altered cell-intrinsic susceptibility to
276 reactivation or if there is a cell-extrinsic influence on reactivation.
277
278 To further interrogate the role of ABCs in controlling latent γHV68 infection, we next asked if
279 mice without ABCs are more susceptible to γHV68 reactivation following infectious challenge.
280 Heterologous viral infection was performed as a physiological mimic to reactivate latent γHV68.
281 Importantly, we chose viruses that do not typically reactivate γHV68[49] such as LCMV and
282 coxsackievirus B4 (CVB4). Specifically, KO and Ctrl mice were infected with γHV68 for 35 days
283 and then challenged with LCMV or CVB4 (Figure 6B). No clinical symptoms were observed
284 during either of the challenges in Ctrl or KO mice. There was no difference in the relative
285 quantity of LCMV and CVB4 in the spleens of Ctrl versus KO mice (Figure 6C-D). Following
286 challenge with LCMV or CVB4, mice lacking ABCs had elevated quantities of γHV68 in the spleen
287 compared to mice with ABCs (Figure 6E-F). We reasoned that the increased γHV68 load
288 following challenge was due to increased reactivation and in support, observed increased
289 relative expression of two lytic-associated γHV68 genes, *Orf50* and *Orf68*, in KO mice compared
290 to Ctrl mice following challenge with the heterologous viruses (Figure 6G-H). Alternatively, we
291 did not observe a difference in expression of the latency-associated gene *Orf73*, between Ctrl

292 and KO mice (Figure 6I).

293

294 Collectively, these findings indicate that mice lacking ABCs are more susceptible to γHV68
295 reactivation and that ABCs play a role in controlling latent γHV68 infection in the face of
296 heterologous challenge.

297

298 ## Discussion

299 Here we have shown that ABCs are increased during acute γHV68 infection and persist during
300 latency for at least 150 days. Previous studies have shown that ABCs persist following clearance
301 of viral infections[8] and during chronic infection[14], though their contribution during a latent
302 infection was unexplored. Our results demonstrate novel role for ABCs: they continuously
303 respond to latent viral infection by secreting anti-viral cytokines and antibodies and play an
304 important role in maintaining γHV68 latency following subsequent infectious challenges.

305

306 Our results show that ABCs continuously expresses anti-viral cytokines during latency and the
307 presence of the latent virus is required for the sustained anti-viral cytokine expression by ABCs.
308 Compared to other B cells, ABCs display uniquely high expression of anti-viral cytokines IFNγ
309 and TNF during γHV68. In addition to expressing cytokines, ABCs also produce anti-viral
310 antibodies, as deficiency of ABCs results in a significant loss of γHV68-specific IgG2c antibodies.
311 We hypothesized that the production of anti-viral cytokines and antibodies by ABCs could be a
312 way in which ABCs monitor and maintain γHV68 latency. Using mice deficient in ABCs, we

showed that ABCs are required for the maintenance of viral latency in the face of heterologous viral challenge.

A surprising finding of our study is that ABCs are increased more so in female than male mice throughout γHV68 infection, in both the blood and spleen. Sex-differences are well-documented in anti-viral immune responses[50] and ABCs have previously been shown to display a female sex bias in contexts of aging and autoimmunity[3,51]. It has recently been shown that the ABC female sex bias in lupus mice is abolished following the duplication of *Tlr7* in male mice[51]. While we show that there is no difference in the quantity of γHV68 between female and male mice, TLR7 stimulation is known to be important for ABC differentiation[2,3] and TLR7 is critical for the control of lytic γHV68 infection and maintenance of latency[52]. While increased frequencies of ABCs were observed in female mice compared to males, we found that a similar proportion of the ABCs express anti-viral cytokines in both males and female mice. No differences between male and female mice were observed in viral load or reactivation.

Our results that the quantity of γHV68 is unchanged in mice with and without ABCs does not align with a previous finding that knocking out ABCs results in an inability to clear γHV68 infection. Rubstova et al. (2013), using bone marrow chimeras to knock out ABCs, report an increased quantity of γHV68 at day 14 p.i. in KO mice compared to controls[5]. We speculate that the observe higher viral load may be due to the additional immunological stress induced by the the irradiation approach required to generate the BM chimera, resulting in increased

334 reactivation. This explanation is in-line with our findings that, without ABCs, mice under stress
335 are more susceptible to γHV68 reactivation and elevated viral loads.
336
337 ABCs are known to possess an array of functional capacities and the precise mechanism(s) of
338 ABC contribution to the control of latent γHV68 infection will be the focus of future studies.
339 Here we have shown that only the antibody response is altered in mice deficient in ABCs and
340 unexpectedly, changes are not observed in the anti-viral T cell response or viral reservoir. The
341 ability of ABCs to provide continuous secretion of anti-viral cytokines is an additional
342 mechanism that likely contributes to the maintenance of γHV68 latency. Understanding the
343 precise localization of ABCs in relation to γHV68-infected B cells will aid in our understanding of
344 the development of splenic structures, in particular germinal centres, as ABCs have been shown
345 to play a role in their development[53].
346
347 Whether ABCs play a role in maintaining latency for human gamma-herpesvirus infections such
348 as Epstein-Barr virus (EBV) and Kaposi sarcoma-associated herpesvirus (KSHV), is not known.
349 Understanding this role would have important relevance in diseases associated with these
350 human gammaherpesviruses, including various malignancies, myalgic
351 encephalomyelitis/chronic fatigue syndrome, and chronic-active EBV[54–56].
352
353 This work demonstrates that ABCs are a long-lasting effector population during γHV68 latency
354 and suggests that they are playing a unique role in the maintenance of latency.
355

356 ## Methods

357

358 ### *Mice*

359 *Tbx21*$^{fl/fl}$*Cd19*$^{cre/+}$ mice were generated by crossing *Tbx21*$^{fl/fl}$*Cd19*$^{cre/+}$ and *Tbx21*$^{fl/fl}$*Cd19*$^{+/+}$ mice.

360 *Tbx21*$^{fl/fl}$ and *Cd19*$^{cre/+}$ mice were provided by Dr. Pippa Marrack[53]. C57BL/6(J) mice were

361 originally purchased from The Jackson Laboratory. All animals were bred and maintained in the

362 animal facility at the University of British Columbia. All animal work was performed per

363 regulations of the Canadian Council for Animal Care (Protocols A17- 0105, A17-0184).

364

365 ### *γHV68, ACRTA-γHV68, and γHV68H2B.YFP infection*

366 γHV68 WUMS strain (ATCC), ACRTA-γHV68 (developed by Dr. Ting-Ting Wu, gift of Dr. Marcia A.

367 Blackman)[29], and γHV68H2B.YFP (developed and provided by Dr. Samuel H. Speck) were

368 propagated in Baby Hamster Kidney cells (BHK, ATCC). Viruses were diluted in Minimum

369 Essential Media (MEM) prior to infection and maintained on ice. 6- to 10-week-old mice were

370 infected i.p. with 10^4 PFU of γHV68, ACRTA-γHV68, γHV68H2B.YFP, or mock-infected with MEM.

371 Clinical symptoms were not observed during γHV68, ACRTA-γHV68, or γHV68H2B.YFP infections

372 in C57BL/6(J) nor *Tbx21*$^{fl/fl}$*Cd19*$^{cre/+}$ or *Tbx21*$^{fl/fl}$*Cd19*$^{+/+}$ mice.

373

374 ### *LCMV infection*

375 LCMV Armstrong strain 53b (originally acquired from Dr. M.B. Oldstone) was propagated on

376 BHK cells. Prior to infection, virus was diluted in RPMI-1640 media (Gibco) and maintained on

377 ice. Mice (11- to 13-week-old) were infected i.p. with 2 x 10^5 PFU LCMV or mock infected with

media. No clinical symptoms were observed from LCMV infection in *Tbx21*$^{fl/fl}$*Cd19*$^{cre/+}$ nor *Tbx21*$^{fl/fl}$*Cd19*$^{+/+}$ mice.

CVB4 infection

CVB4 Edward strain was propagated on HeLa cells and titred by plaque assay. Virus was diluted in Dulbecco's Modified Eagle Medium (DMEM, Gibco) and maintained on ice prior to infection. Mice (11- to -13-week-old) were infected i.p. with 100 PFU CBV4. No clinical symptoms were observed from CVB4 infection in *Tbx21*$^{fl/fl}$*Cd19*$^{cre/+}$ or *Tbx21*$^{fl/fl}$*Cd19*$^{+/+}$ mice.

Tissue harvesting and processing for flow cytometry

Mice were anesthetised with isoflurane and euthanized by cardiac puncture. For flow cytometry, blood was collected by cardiac puncture into 100 ul 0.5 M Ethylenediaminetetraacetic acid (EDTA) to prevent clotting and placed on ice until processing. Spleen extracted and placed into 2 ml PBS and kept on ice until processing. Blood was incubated in 10 ml warmed (37°C) ACK lysis buffer for 15 minutes at room temperature to remove red blood cells and washed twice with FACS buffer. Spleens were mashed through a 70 µm cell strainer with a 3 ml syringe insert to make a single cell suspension for each sample. Splenocytes were incubated in 4 ml warmed (37°C) ACK lysis buffer for 10 minutes on ice to lyse red blood cells and remaining cells were resuspended in FACS buffer and kept on ice until further use.

Flow cytometry analysis of cell-type specific surface antigens and intracellular cytokines

400 For analysis of extracellular and intracellular antigens, 2 million cells per spleen sample or all
401 cells collected per blood sample were stained with appropriate antibodies. Prior to staining,
402 samples were incubated at 4°C covered from light for 30 minutes with 2 µl/ml Fixable Viability
403 Dye eFluor506 (Thermo Fisher) while in PBS and then resuspended in rat anti-mouse CD16/32
404 (Fc block, BD Biosciences) antibody for 10 minutes. Then, samples were stained with
405 fluorochrome labeled antibodies (Table 1) against cell surface antigens for 30 minutes covered
406 from light at 4°C, washed, and resuspended in Fix/Perm buffer (Thermo Fisher) for 30 minutes-
407 12 hours while maintained covered from light at 4°C. Samples were then washed twice with
408 perm buffer and incubated 40 minutes with antibodies for intracellular antigens (Table 1) in
409 Perm buffer at covered from light at RT. Cells were then washed and resuspended in FACS
410 buffer with 2 mM EDTA. For analysis of cytokine production, 4 million cells per sample were
411 stimulated ex vivo for 3 hours at 5% CO2 at 37°C in Minimum Essential Media (Gibco)
412 containing 10% fetal bovine serum (FBS, Sigma-Aldrich), 1 µl/ml GolgiPlug (BD Biosciences), 10
413 ng/ml PMA (Sigma-Aldrich) and 500 ng/ml ionomycin (Thermo Fisher) and washed prior to
414 staining. Samples were collected on an Attune NxT Flow Cytometer (Thermo Fisher) and
415 analyzed with FlowJo software v10 (FlowJo LLC).
416

Antigen	Fluor	Clone	Dilution	Company
CD3e	eFluor 450	500A2	1:200	Thermo Fisher Scientific
CD19	PE	1D3	1:200	Thermo Fisher Scientific
CD19	Pe-Cy7	1D3	1:200	Thermo Fisher Scientific
CD19	SB780	1D3	1:100	Thermo Fisher Scientific
IgD	Pe-Cy7	11-26	1:200	Thermo Fisher Scientific
CD11c	Alexafluor700	N418	1:100	Thermo Fisher Scientific
CD11c	APC	N418	1:100	Biolegend
T-bet	PerCpCy5.5	4B10	1:100	Thermo Fisher Scientific
IFNγ	APC	XMG1.2	1:100	Thermo Fisher Scientific

TNF	Pe-Cy7	MP6-XT22	1:100	Biolegend
IL-17A	PEDazzle594	TC11-18H10.1	1:100	Biolegend
CD45	Alexafluor700	30-F11	1:200	Thermo Fisher Scientific
CD45	APC-eFluor 780	30-F11	1:200	Thermo Fisher Scientific
CD4	SB645	RM4-5	1:100	Thermo Fisher Scientific
CD8	APC-eFluor 780	53-6.7	1:200	Thermo Fisher Scientific
CD8	PEDazzle594	53-6.7	1:100	Biolegend
CD11b	Pe-Cy7	M1/70	1:100	Thermo Fisher Scientific
Ly6G	PerCpCy5.5	RB6-8C5	1:100	Thermo Fisher Scientific
CD335	FitC	29A1.4	1:100	Thermo Fisher Scientific
NK1.1	PE	PK136	1:100	Thermo Fisher Scientific
F4/80	APC-eFluor 780	BM8	1:100	Thermo Fisher Scientific
CD62L	PerCpCy5.5	MEL-14	1:100	Thermo Fisher Scientific
CD44	Alexafluor700	IM7	1:200	Thermo Fisher Scientific
PD1	PerCpeFluor 710	RMP1-30	1:100	Thermo Fisher Scientific
CXCR5	PE	SPRCL5	1:100	Thermo Fisher Scientific
FoxP3	Alexafluor700	FJK-16s	1:100	Thermo Fisher Scientific
CD138	PEDazzle594	281-2	1:100	Biolegend
CD95	FitC	SA367H8	1:100	Biolegend
IgM	APCCy7	RMM-1	1:100	Biolegend
TCR Vβ4	FitC	KT4	1:100	BD Bioscience

Table 1 Flow cytometry antibodies

Tetramer staining

γHV68-specific CD8 T cells were identified by staining with a tetramer acquired from the NIH Tetramer Facility. 2 million cells per well were incubated for 1 hour at RT with p79 (K^b/ORF61$_{524–531}$ TSINFVKI, diluted 1:400) following viability staining and Fc receptor block, as described above, but before extracellular antigen staining. Uninfected mice stained with tetramers used as negative gating controls.

425

426 *γHV68 qPCR*

427 DNA was isolated from 4 x 10^6 splenocytes using PureLink™ Genomic DNA Mini Kit (Thermo
428 Fisher) and quantified with a spectrophotometer. qPCR was performed using 2x QuantiNova
429 Probe Mastermix (Qiagen, USA) on the Bio-Rad CFX96 Touch™ Real Time PCR Detection system.
430 Copies of γHV68 were quantified in duplicate wells with 150 ng DNA per reaction using primers
431 and probes specific to γHV68 *Orf50* and mouse *Ptger2* (Table 2). Standard curves were obtained
432 by serial dilutions of *Orf50* and *Ptger2* gBlocks (*Orf50*: $2x10^6$ – $2x10^1$; *Ptger2*: $5x10^7$-$5x10^2$) that
433 were amplified in parallel.

434
435

Gene	Sequence
Ptger2 Forward Primer	5′-TACCTTCAGCTGTACGCCAC-3′
Ptger2 Reverse Primer	5′-GCCAGGAGAATGAGGTGGTC-3′
Ptger2 Probe	5′-/56-FAM/CCTGCTGCT/ZEN/TATCGTGGCTG/3IABkFQ/-3′
Orf50 Forward Primer	5′-TGGACTTTGACAGCCCAGTA-3′
Orf50 Reverse Primer	5′- TCCCTTGAGGCAAATGATTC-3′
Orf50 Probe	5′-/56-FAM/TGACAGTGC/ZEN/CTATGGCCAAGTCTTG/3IABkFQ/-3′

436 Table 2 γHV68 qPCR primers and probe sequences

437

438 *RT-qPCR for γHV68 lytic and latency-associated genes and relative quantity of LCMV and CVB4*

439 Portion of spleen stabilized in RNAlater immediately following collection and stored at -80°C for
440 up to 12 weeks. RNA extracted with RNeasy mini kit (Qiagen, cat no. 74104) and cDNA
441 immediately synthesized with High-Capacity cDNA Reverse Transcription Kit (Thermo Fisher, cat

442 no. 4368814). Reaction performed with 500ng per reaction in duplicate wells. cDNA quantified
443 with a spectrophotometer. qPCR was performed using iQTM SYBR® Green supermix (Bio-Rad)
444 on the Bio-Rad CFX96 Touch™ Real Time PCR Detection system. Transcript specific primers have
445 been previously described for *Orf50*, *Orf73*, and *Orf68*[57], LCMV[58], and CVB4[59]. Primers were
446 ordered from Integrated DNA Technologies (Table 3). Normalized to the ribosomal
447 housekeeping gene *18s* and expression determined relative to control group.

448

Gene	Sequence
Orf50 forward	5'-GGCCGCAGACATTTAATGAC-3'
Orf50 reverse	5'-GCCTCAACTTCTCTGGATATGCC-3'
Orf73 forward	5'-AAGGGTTGTCTTGGCCTAC TGTG-3'
Orf73 reverse	5'-AGAGATGCTGTGGGACCATGTTG-3'
Orf68 forward	5'-CTCAAATACACTGGCCGCCATC-3'
Orf68 reverse	5'-CGTGCTTGAGATATGAGTGAGT-3'
CVB4 forward	5'-CCCACAGGACGCTCTAATA-3'
CVB4 reverse	5'-CAGAGTTACCCGTTACGACA -3'
LCMV GP forward	5'-TGCCTGACCAAATGGATGATT-3'
LCMV GP reverse	5'-CTGCTGTGTTCCCGAAACACT-3'
18s forward	5'-GTAACCCGTTGAACCCCATT-3'
18s reverse	5'-CCATCCAATCGGTAGTAGCG-3'

449 Table 3 qPCR for lytic and latent γHV68 genes primer sequences

450 *Ex vivo limiting dilution reactivation assay*

451 A single cell suspension following RBC lysis with ACK lysis buffer was prepared from freshly
452 collected spleens. To analyze ex vivo reactivation, limiting dilution reactivation assay was
453 performed as previously described[16]. Two-fold serial dilutions of splenocytes starting at 10^5
454 cells per well were plated onto monolayer of mouse embryonic fibroblast (MEF, C57BL/6) cells
455 (ATCC) in 96-well flat-bottom polystyrene tissue culture plates. Twelve wells were plated per
456 dilution. Plates were incubated at 37°C 5% CO_2 for 10 days and scored for microscopically for
457 viral cytopathic effects (CPE).

458

459 *Anti-γHV68 antibodies*

460 Serum was collected via cardiac puncture and maintained at RT to allow for clotting. The sera
461 were isolated by centrifugation 2000 × g for 10 min, aliquoted, and stored for up to 12 months
462 at -80°C prior to running the ELISA. Anti-γHV68 antibodies were quantified by standard indirect
463 ELISA. Briefly, γHV68 virions were inactivated in 4% paraformaldehyde (PFA) for 20 minutes at
464 RT. Then, ELISA plates (NUNC, Thermo Fisher) were coated with 5 µg/ml γHV68 in coating
465 buffer (0.05 M $NaHCO_3$, pH 9.6) with 1% PFA overnight at 4°C. Continue. The plate was then
466 washed 4x with wash buffer (PBS-0.05% Tween-20), blocked in blocking buffer (5% NBCS in PBS)
467 for 1 hour at 37°C, and incubated with serial dilutions (1:20, 1:40, 1:80, 1:160, 1:320, 1:640,
468 1:1280, 1:2560) of test sera diluted in blocking buffer for 2 hours at 37°C. The plate was washed
469 4x with wash buffer and bound antibody was incubated with HRP-conjugated goat anti-mouse
470 IgG (Thermo Fisher), rat anti-mouse IgG1 (BD Biosciences), or goat anti-mouse IgG2c (Thermo
471 Fisher), all diluted 1:500 in blocking buffer, for 1 hour at 37°C, washed 4x with wash buffer, and
472 detected by TMB substrate (BD Biosciences). Absorbance was read at 450 nm on a VarioSkan
473 Plate Reader (Thermo Fisher).

474

475 *Statistical analyses*

476 Data analysis and presentation as well as statistical tests were performed using GraphPad Prism
477 software 8.4.2 (GraphPad Software Inc.). Results are presented as mean ± SEM. Statistical
478 tests, significance (p-value), sample size (n, number of mice per group) and number of
479 experimental replicates are stated in the figure legends. Statistical analyses included: two-way

ANOVA with Geisser-Greenhouse's correction, Mann-Whitney test, and one-way ANOVA. P-values indicated by asterisks as follows: ****$p<0.0001$, *** $p<0.001$, ** $p<0.01$, * $p<0.05$.

Study approval

All work was approved by the Animal Care Committee (ACC) of the University of British Columbia (Protocols A17- 0105, A17-0184).

Acknowledgements

The following reagent was obtained through the NIH Tetramer Core Facility: class I p79 tetramer. The authors thank Martin Richer for the helpful feedback on the manuscript.

References

1. Barton E, Mandal P, Speck SH. Pathogenesis and host control of gammaherpesviruses: lessons from the mouse. *Annu Rev Immunol*. 2011;29:351-397. doi:10.1146/annurev-immunol-072710-081639

2. Hao Y, O'Neill P, Naradikian MS, Scholz JL, Cancro MP. A B-cell subset uniquely responsive to innate stimuli accumulates in aged mice. *Blood*. 2011;118(5):1294-1304. doi:10.1182/blood-2011-01-330530

3. Rubtsov AV, Rubtsova K, Fischer A, et al. Toll-like receptor 7 (TLR7)–driven accumulation of a novel CD11c+ B-cell population is important for the development of autoimmunity. *Blood*. 2011;118(5):1305-1315. doi:10.1182/blood-2011-01-331462

4. Cancro MP. Age-Associated B Cells. *Annu Rev Immunol*. 2020;38(1):315-340. doi:10.1146/annurev-immunol-092419-031130

5. Rubtsova K, Rubtsov AV, Dyk LF van, Kappler JW, Marrack P. T-box transcription factor T-bet, a key player in a unique type of B-cell activation essential for effective viral clearance. *Proc Natl Acad Sci*. 2013;110(34):E3216-E3224. doi:10.1073/pnas.1312348110

6. Rubtsova K, Rubtsov AV, Halemano K, et al. T Cell Production of IFNγ in Response to TLR7/IL-12 Stimulates Optimal B Cell Responses to Viruses. *PloS One*. 2016;11(11):e0166322. doi:10.1371/journal.pone.0166322

7. Knox JJ, Buggert M, Kardava L, et al. T-bet+ B cells are induced by human viral infections and dominate the HIV gp140 response. *JCI Insight*. 2017;2(8). doi:10.1172/jci.insight.92943

8. Johnson JL, Rosenthal RL, Knox JJ, et al. The Transcription Factor T-bet Resolves Memory B Cell Subsets with Distinct Tissue Distributions and Antibody Specificities in Mice and Humans. *Immunity*. April 2020. doi:10.1016/j.immuni.2020.03.020

9. Eccles JD, Turner RB, Kirk NA, et al. T-bet+ Memory B Cells Link to Local Cross-Reactive IgG upon Human Rhinovirus Infection. *Cell Rep*. 2020;30(2):351-366.e7. doi:10.1016/j.celrep.2019.12.027

10. Woodruff MC, Ramonell RP, Nguyen DC, et al. Extrafollicular B cell responses correlate with neutralizing antibodies and morbidity in COVID-19. *Nat Immunol*. 2020;21(12):1506-1516. doi:10.1038/s41590-020-00814-z

11. Rubtsov AV, Rubtsova K, Kappler JW, Jacobelli J, Friedman RS, Marrack P. CD11c-Expressing B Cells Are Located at the T Cell/B Cell Border in Spleen and Are Potent APCs. *J Immunol Baltim Md 1950*. 2015;195(1):71-79. doi:10.4049/jimmunol.1500055

524 12. Mendoza A, Yewdell WT, Hoyos B, et al. Assembly of a spatial circuit of T-bet–expressing T
525 and B lymphocytes is required for antiviral humoral immunity. *Sci Immunol*. 2021;6(60).
526 doi:10.1126/sciimmunol.abi4710

527 13. Peng SL, Szabo SJ, Glimcher LH. T-bet regulates IgG class switching and pathogenic
528 autoantibody production. *Proc Natl Acad Sci U S A*. 2002;99(8):5545-5550.
529 doi:10.1073/pnas.082114899

530 14. Barnett BE, Staupe RP, Odorizzi PM, et al. B cell intrinsic T-bet expression is required to
531 control chronic viral infection. *J Immunol Baltim Md 1950*. 2016;197(4):1017-1022.
532 doi:10.4049/jimmunol.1500368

533 15. Ehtisham S, Sunil-Chandra NP, Nash AA. Pathogenesis of murine gammaherpesvirus
534 infection in mice deficient in CD4 and CD8 T cells. *J Virol*. 1993;67(9):5247-5252.
535 doi:10.1128/JVI.67.9.5247-5252.1993

536 16. Weck KE, Barkon ML, Yoo LI, Speck SH, Virgin HW IV. Mature B cells are required for acute
537 splenic infection, but not for establishment of latency, by murine gammaherpesvirus 68. *J*
538 *Virol*. 1996;70(10):6775-6780. doi:10.1128/JVI.70.10.6775-6780.1996

539 17. Willer DO, Speck SH. Long-Term Latent Murine Gammaherpesvirus 68 Infection Is
540 Preferentially Found within the Surface Immunoglobulin D-Negative Subset of Splenic B
541 Cells In Vivo. *J Virol*. 2003;77(15):8310-8321. doi:10.1128/JVI.77.15.8310-8321.2003

542 18. Simas JP, Swann D, Bowden R, Efstathiou S. Analysis of murine gammaherpesvirus-68
543 transcription during lytic and latent infection. *J Gen Virol*. 1999;80 (Pt 1):75-82.
544 doi:10.1099/0022-1317-80-1-75

545 19. Kim IJ, Flaño E, Woodland DL, Blackman MA. Antibody-mediated control of persistent
546 gamma-herpesvirus infection. *J Immunol Baltim Md 1950*. 2002;168(8):3958-3964.
547 doi:10.4049/jimmunol.168.8.3958

548 20. Freeman ML, Burkum CE, Woodland DL, Sun R, Wu TT, Blackman MA. Importance of
549 antibody in virus infection and vaccine-mediated protection by a latency-deficient
550 recombinant murine γ-herpesvirus-68. *J Immunol Baltim Md 1950*. 2012;188(3):1049-
551 1056. doi:10.4049/jimmunol.1102621

552 21. Stevenson PG, Cardin RD, Christensen JP, Doherty PC. Immunological control of a murine
553 gammaherpesvirus independent of CD8+ T cells. *J Gen Virol*. 1999;80 (Pt 2):477-483.
554 doi:10.1099/0022-1317-80-2-477

555 22. Steed A, Buch T, Waisman A, Virgin HW. Gamma Interferon Blocks Gammaherpesvirus
556 Reactivation from Latency in a Cell Type-Specific Manner. *J Virol*. 2007;81(11):6134-6140.
557 doi:10.1128/JVI.00108-07

558 23. Goodwin MM, Canny S, Steed A, Virgin HW. Murine gammaherpesvirus 68 has evolved
559 gamma interferon and stat1-repressible promoters for the lytic switch gene 50. *J Virol*.
560 2010;84(7):3711-3717. doi:10.1128/JVI.02099-09

561 24. Stewart JP, Usherwood EJ, Ross A, Dyson H, Nash T. Lung Epithelial Cells Are a Major Site
562 of Murine Gammaherpesvirus Persistence. *J Exp Med*. 1998;187(12):1941-1951.

563 25. Usherwood EJ, Stewart JP, Robertson K, Allen DJ, Nash AA. Absence of splenic latency in
564 murine gammaherpesvirus 68-infected B cell-deficient mice. *J Gen Virol*. 1996;77 (Pt
565 11):2819-2825. doi:10.1099/0022-1317-77-11-2819

566 26. Weck KE, Kim SS, Virgin HW, Speck SH. B Cells Regulate Murine Gammaherpesvirus 68
567 Latency. *J Virol*. 1999;73(6):4651-4661.

568 27. Siegel AM, Rangaswamy US, Napier RJ, Speck SH. Blimp-1-Dependent Plasma Cell
569 Differentiation Is Required for Efficient Maintenance of Murine Gammaherpesvirus
570 Latency and Antiviral Antibody Responses. *J Virol*. 2010;84(2):674-685.
571 doi:10.1128/JVI.01306-09

572 28. Mouat IC, Allanach JR, Fan V, et al. *Gammaherpesvirus Infection Licenses Age-Associated B*
573 *Cells for Pathogenicity in MS and EAE*.; 2021:2021.07.22.453263.
574 doi:10.1101/2021.07.22.453263

575 29. Jia Q, Freeman ML, Yager EJ, et al. Induction of Protective Immunity against Murine
576 Gammaherpesvirus 68 Infection in the Absence of Viral Latency. *J Virol*. 2010;84(5):2453-
577 2465. doi:10.1128/JVI.01543-09

578 30. Flaño E, Husain SM, Sample JT, Woodland DL, Blackman MA. Latent murine gamma-
579 herpesvirus infection is established in activated B cells, dendritic cells, and macrophages. *J*
580 *Immunol Baltim Md 1950*. 2000;165(2):1074-1081. doi:10.4049/jimmunol.165.2.1074

581 31. Sunil-Chandra NP, Efstathiou S, Nash AA. Murine gammaherpesvirus 68 establishes a
582 latent infection in mouse B lymphocytes in vivo. *J Gen Virol*. 1992;73 (Pt 12):3275-3279.
583 doi:10.1099/0022-1317-73-12-3275

584 32. Marques S, Efstathiou S, Smith KG, Haury M, Simas JP. Selective Gene Expression of Latent
585 Murine Gammaherpesvirus 68 in B Lymphocytes. *J Virol*. 2003;77(13):7308-7318.
586 doi:10.1128/JVI.77.13.7308-7318.2003

587 33. Collins CM, Boss JM, Speck SH. Identification of Infected B-Cell Populations by Using a
588 Recombinant Murine Gammaherpesvirus 68 Expressing a Fluorescent Protein. *J Virol*.
589 2009;83(13):6484-6493. doi:10.1128/JVI.00297-09

590 34. Collins CM, Speck SH. Tracking murine gammaherpesvirus 68 infection of germinal center
591 B cells in vivo. *PloS One*. 2012;7(3):e33230. doi:10.1371/journal.pone.0033230

592 35. Staudt MR, Dittmer DP. The Rta/Orf50 transactivator proteins of the gamma-
593 herpesviridae. *Curr Top Microbiol Immunol*. 2007;312:71-100. doi:10.1007/978-3-540-
594 34344-8_3

595 36. Didychuk AL, Gates SN, Gardner MR, Strong LM, Martin A, Glaunsinger BA. A pentameric
596 protein ring with novel architecture is required for herpesviral packaging. Carter AP,
597 Wolberger C, Graham SC, eds. *eLife*. 2021;10:e62261. doi:10.7554/eLife.62261

598 37. Fowler P, Marques S, Simas JP, Efstathiou S. ORF73 of murine herpesvirus-68 is critical for
599 the establishment and maintenance of latency. *J Gen Virol*. 2003;84(Pt 12):3405-3416.
600 doi:10.1099/vir.0.19594-0

601 38. Moorman NJ, Willer DO, Speck SH. The gammaherpesvirus 68 latency-associated nuclear
602 antigen homolog is critical for the establishment of splenic latency. *J Virol*.
603 2003;77(19):10295-10303. doi:10.1128/jvi.77.19.10295-10303.2003

604 39. Wang G, Zarek C, Chang T, Tao L, Lowe A, Reese TA. Th2 Cytokine Modulates Herpesvirus
605 Reactivation in a Cell Type Specific Manner. *J Virol*. February 2021:JVI.01946-20.
606 doi:10.1128/JVI.01946-20

607 40. Barton ES, White DW, Cathelyn JS, et al. Herpesvirus latency confers symbiotic protection
608 from bacterial infection. *Nature*. 2007;447(7142):326-329. doi:10.1038/nature05762

609 41. Tibbetts SA, van Dyk LF, Speck SH, Virgin HW. Immune Control of the Number and
610 Reactivation Phenotype of Cells Latently Infected with a Gammaherpesvirus. *J Virol*.
611 2002;76(14):7125-7132. doi:10.1128/JVI.76.14.7125-7132.2002

612 42. Gredmark-Russ S, Cheung EJ, Isaacson MK, Ploegh HL, Grotenbreg GM. The CD8 T-Cell
613 Response against Murine Gammaherpesvirus 68 Is Directed toward a Broad Repertoire of
614 Epitopes from both Early and Late Antigens. *J Virol*. 2008;82(24):12205-12212.
615 doi:10.1128/JVI.01463-08

616 43. Steed AL, Barton ES, Tibbetts SA, et al. Gamma Interferon Blocks Gammaherpesvirus
617 Reactivation from Latency. *J Virol*. 2006;80(1):192-200. doi:10.1128/JVI.80.1.192-200.2006

618 44. Dutia BM, Clarke CJ, Allen DJ, Nash AA. Pathological changes in the spleens of gamma
619 interferon receptor-deficient mice infected with murine gammaherpesvirus: a role for CD8
620 T cells. *J Virol*. 1997;71(6):4278-4283.

621 45. Tripp RA, Hamilton-Easton AM, Cardin RD, et al. Pathogenesis of an Infectious
622 Mononucleosis-like Disease Induced by a Murine γ-Herpesvirus: Role for a Viral
623 Superantigen? *J Exp Med*. 1997;185(9):1641-1650.

624 46. Hardy CL, Flaño E, Cardin RD, et al. Factors controlling levels of CD8+ T-cell lymphocytosis
625 associated with murine gamma-herpesvirus infection. *Viral Immunol*. 2001;14(4):391-402.
626 doi:10.1089/08828240152716637

627 47. Evans AG, Moser JM, Krug LT, Pozharskaya V, Mora AL, Speck SH. A gammaherpesvirus-
628 secreted activator of Vbeta4+ CD8+ T cells regulates chronic infection and
629 immunopathology. *J Exp Med*. 2008;205(3):669-684. doi:10.1084/jem.20071135

630 48. Stevenson PG, Belz GT, Altman JD, Doherty PC. Changing patterns of dominance in the
631 CD8+ T cell response during acute and persistent murine gamma-herpesvirus infection. *Eur*
632 *J Immunol*. 1999;29(4):1059-1067. doi:10.1002/(SICI)1521-4141(199904)29:04<1059::AID-
633 IMMU1059>3.0.CO;2-L

634 49. Barton ES, Rajkarnikar S, Langston PK, Price MJ, Grayson JM. Gammaherpesvirus latency
635 differentially impacts the generation of primary versus secondary memory CD8+ T cells
636 during subsequent infection. *J Virol*. 2014;88(21):12740-12751. doi:10.1128/JVI.02106-14

637 50. Jacobsen H, Klein SL. Sex Differences in Immunity to Viral Infections. *Front Immunol*.
638 2021;12:3483. doi:10.3389/fimmu.2021.720952

639 51. Ricker E, Manni M, Flores-Castro D, et al. Altered function and differentiation of age-
640 associated B cells contribute to the female bias in lupus mice. *Nat Commun*.
641 2021;12(1):4813. doi:10.1038/s41467-021-25102-8

642 52. Bussey KA, Murthy S, Reimer E, et al. Endosomal Toll-Like Receptors 7 and 9 Cooperate in
643 Detection of Murine Gammaherpesvirus 68 Infection. *J Virol*. 2019;93(3):e01173-18.
644 doi:10.1128/JVI.01173-18

645 53. Rubtsova K, Rubtsov AV, Thurman JM, Mennona JM, Kappler JW, Marrack P. B cells
646 expressing the transcription factor T-bet drive lupus-like autoimmunity. *J Clin Invest*.
647 2017;127(4):1392-1404. doi:10.1172/JCI91250

648 54. Vockerodt M, Yap LF, Shannon-Lowe C, et al. The Epstein-Barr virus and the pathogenesis
649 of lymphoma. *J Pathol*. 2015;235(2):312-322. doi:10.1002/path.4459

650 55. Shikova E, Reshkova V, Kumanova A, et al. Cytomegalovirus, Epstein-Barr virus, and human
651 herpesvirus-6 infections in patients with myalgic encephalomyelitis/chronic fatigue
652 syndrome. *J Med Virol*. March 2020. doi:10.1002/jmv.25744

653 56. Tsuge I, Morishima T, Kimura H, Kuzushima K, Matsuoka H. Impaired cytotoxic T
654 lymphocyte response to Epstein-Barr virus-infected NK cells in patients with severe
655 chronic active EBV infection. *J Med Virol*. 2001;64(2):141-148. doi:10.1002/jmv.1029

656 57. Abernathy E, Clyde K, Yeasmin R, et al. Gammaherpesviral gene expression and virion
657 composition are broadly controlled by accelerated mRNA degradation. *PLoS Pathog*.
658 2014;10(1):e1003882. doi:10.1371/journal.ppat.1003882

659 58. Welsh RM, Seedhom MO. LCMV: Propagation, quantitation, and storage. *Curr Protoc*
660 *Microbiol*. 2008;CHAPTER:Unit-15A.1. doi:10.1002/9780471729259.mc15a01s8

59. Walter DL, Benner SE, Oaks RJ, et al. Coxsackievirus B4 Exposure Results in Variable Pattern Recognition Response in the Kidneys of Female Non-Obese Diabetic Mice Before Establishment of Diabetes. *Viral Immunol*. 2020;33(7):494-506. doi:10.1089/vim.2019.0188

666 **Figure 1**

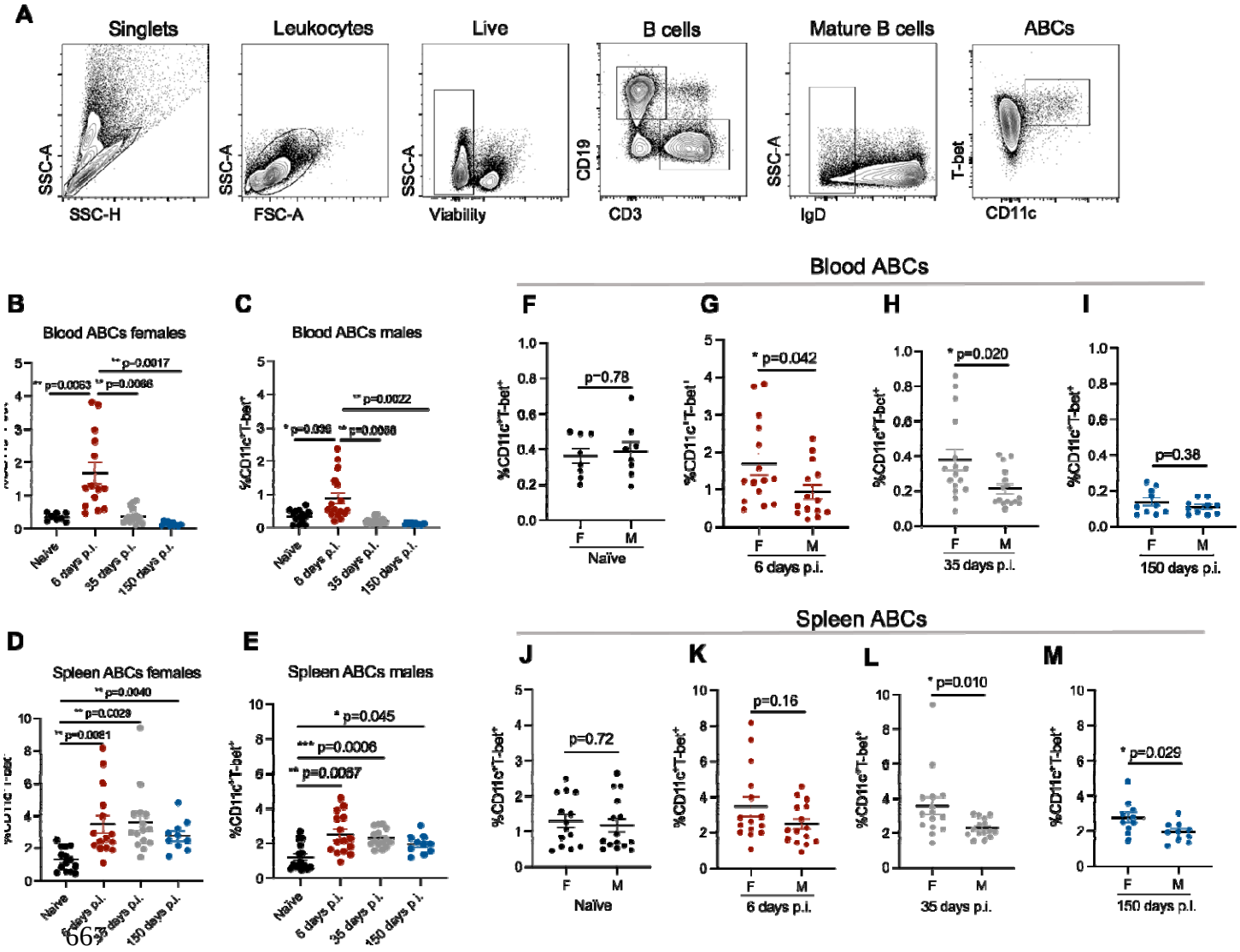

667
668

Figure 1 ABCs expand in the blood and spleen throughout γHV68 infection

Blood and spleen collected from C57BL/6(J) mice (6–8-week-old at infection) mock-infected with media (naïve, black circles) or infected i.p. with γHV68 for 6 (red circles), 35 (grey circles), or 150 (blow circles) days and processed for flow cytometry. **(A)** Representative gating strategy of ABCs. IgD, CD11c, and T-bet gating used fluorescence-minus-one (FMO) controls. (**B-E**) Proportion of ABCs ($CD11c^{+}T\text{-}bet^{+}$) of mature B cells ($CD19^{+}IgD^{-}$) in the blood and spleen of male and female mice. (**F-I**) Proportion of ABCs ($CD11c^{+}T\text{-}bet^{+}$) of mature B cells ($CD19^{+}IgD^{-}$) in the blood or spleen of male and female mice. Same data as presented in panels B-E. n=10-15 mice per group, data compiled from 4 experiments. Each data point represents an individual mouse. Data presented as mean ± SEM. Analyzed by (**B-E**) one-way ANOVA or (**F-M**) Mann-Whitney test. P-values indicated as asterixis as follows: *** $p<0.001$, ** $p<0.01$, * $p<0.05$.

681 **Figure 2**

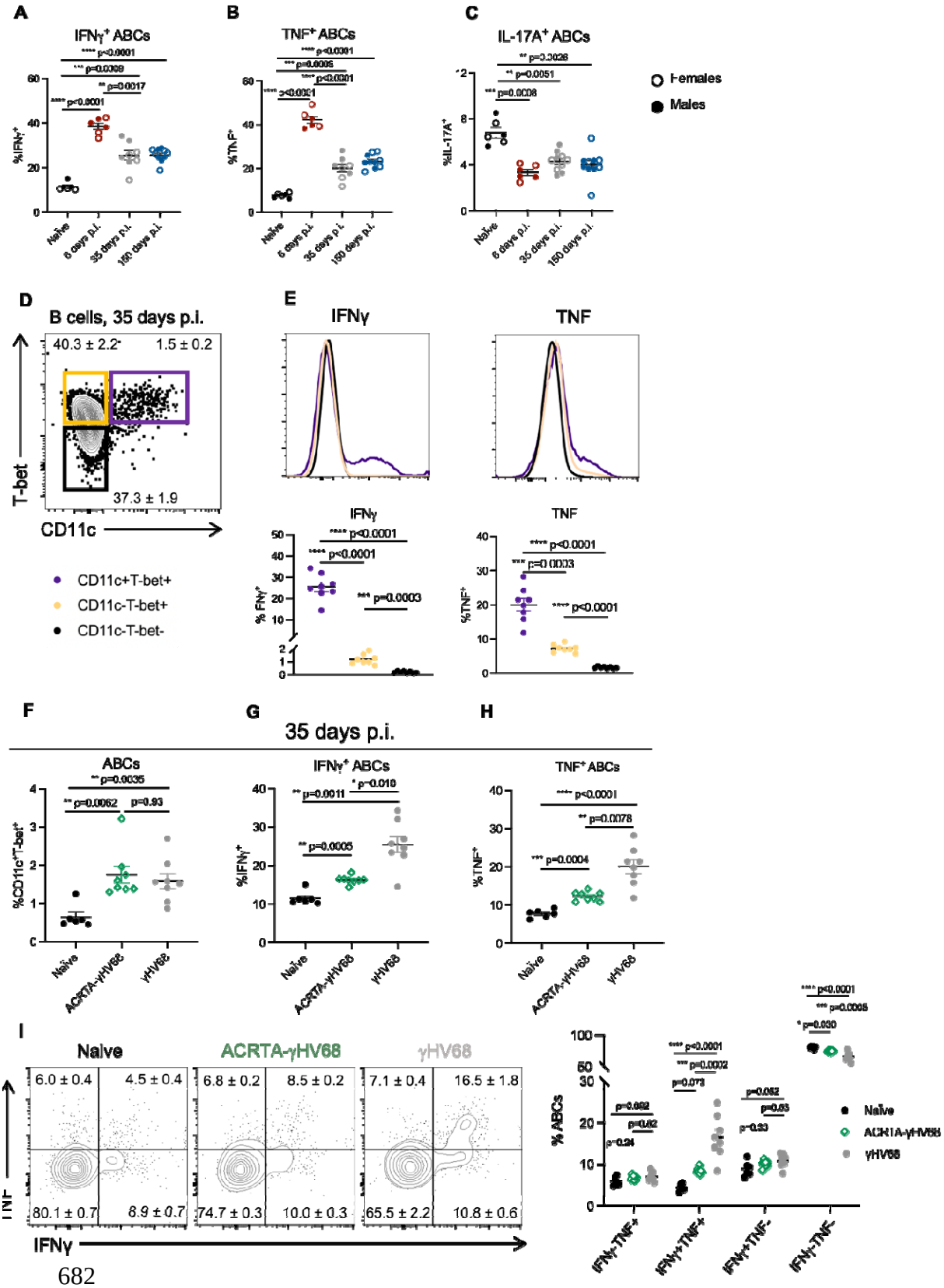

682

Figure 2 Cytokine production by ABCs in the spleen during γHV68 and ACRTA-γHV68 infection

(**A-C**) C57BL/6(J) mice (6–8-week-old at infection) mock-infected with media (naïve) or infected i.p. with γHV68 for 6, 35, or 150 days. Spleens collected and processed for flow cytometry. Proportion of ABCs in the spleen expressing (**A**) IFNγ, (**B**) TNF, or (**C**) IL-17A, with females presented as open circles and males as filled circles. (**D**) Gating of ABCs ($CD11c^{+}T\text{-}bet^{+}$) and non-ABC B cells ($CD11c^{-}T\text{-}bet^{+}$ and $CD11c^{-}T\text{-}bet^{-}$), previously gated on $CD19^{+}IgD^{-}$ cells in the spleen. (**E**) Representative histograms and dot plots of the proportion of ABCs and non-ABC B cells ($CD11c^{-}T\text{-}bet^{+}$ and $CD11c^{-}T\text{-}bet^{-}$) expressing IFNγ and TNF from mice infected with γHV68 for 35 days. (**F-H**) C57BL/6(J) mice mock-infected with media (Naïve, black circles) or infected i.p. with γHV68 (grey circles) or ACRTA-γHV68 (green diamonds) for 35 days and spleens processed for flow cytometry. (**F**) Proportion of ABCs ($CD11c^{+}T\text{-}bet^{+}$) of mature B cells ($CD19^{+}IgD^{-}$) in the spleen. Proportion of ABCs ($CD19^{+}CD11c^{+}T\text{-}bet^{+}$) in the spleen expressing (**G**) IFNγ or (**H**) TNF. (**I**) Representative plots and quantification of the proportion of ABCs expressing IFNγ and TNF. Equivalent numbers of females and per group in all panels. (**A-C**) n=6-10 mice per group, data combined from two experiments. (**E-I**) n=6-8 mice per group, representative of two experiments. Each data point represents an individual mouse. Data presented as mean ± SEM. Analyzed by one-way ANOVA. P-values indicated as asterixis as follows: ****$p<0.0001$, *** $p<0.001$, ** $p<0.01$, * $p<0.05$.

702 **Figure 3**

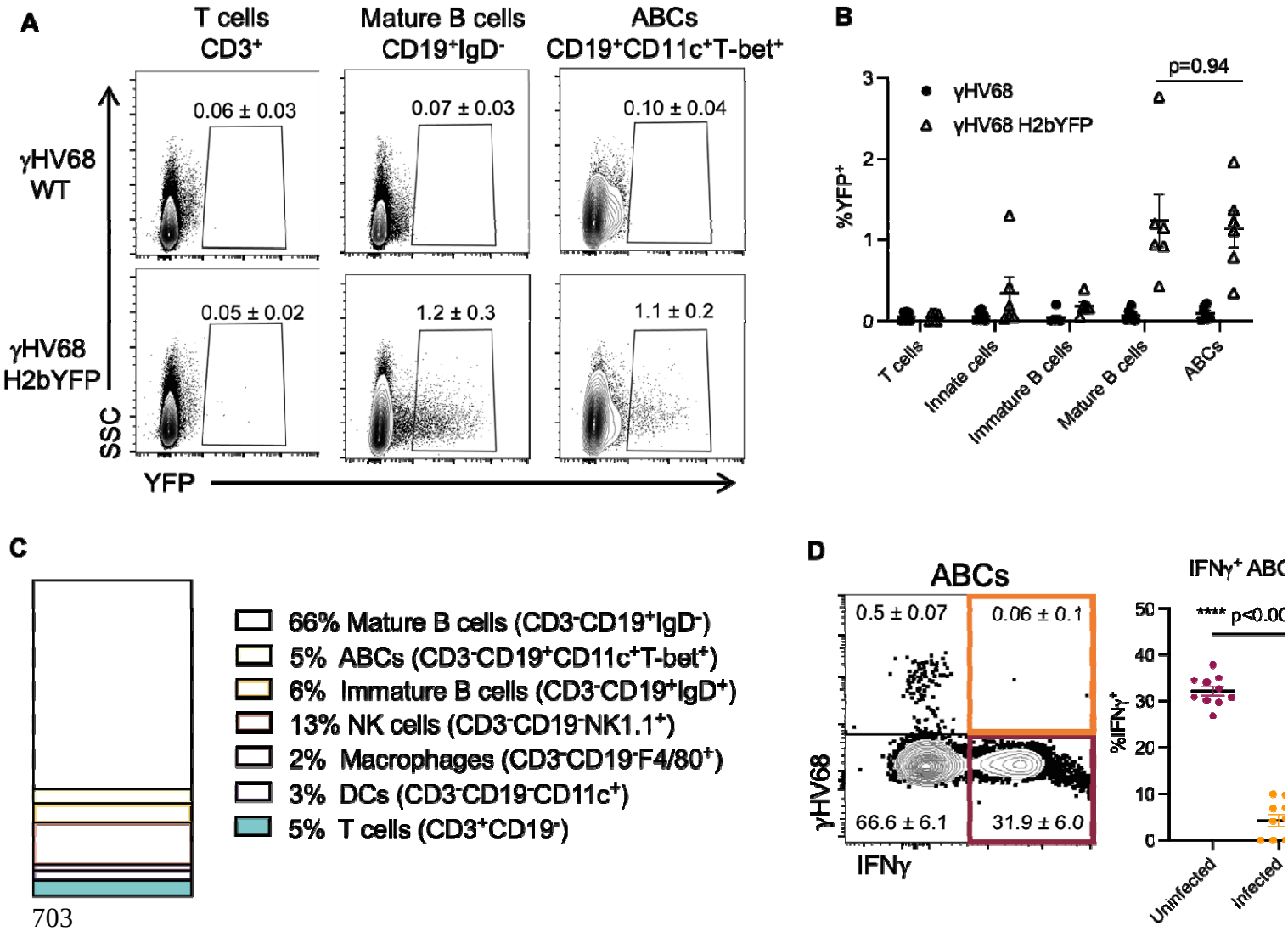

703
704

Figure 3 Analysis of ABC infection status with fluorescent γHV68 strain

Female C57BL/6(J) mice (6 to 8-week-old at infection) infected i.p. with γHV68 or γHV68.H2bYFP. 8 days p.i. spleen collected and processed for flow cytometry. (**A**) Representative flow cytometry plots displaying yellow fluorescent protein (YFP) expression (x-axis) versus side-scatter (SSC, y-axis) from mice infected with γHV68 or γHV68.H2bYFP with mean ± SEM. Samples gated on live, single lymphocytes, and then T cells ($CD3^+$), total B cells ($CD19^+$), mature B cells ($CD19^+IgD^-$), or ABCs ($CD19^+CD11c^+T\text{-}bet^+$). Samples concatenated from one experiment, representative of two experiments. (**B**) Proportion of cell subsets positive for YFP expression from γHV68-infected mice (filled circles) and γHV68.H2bYFP-infected mice (open triangles). Each data point represents an individual mouse. (**C**) Proportion of YFP^+ cells that are non-B cells ($CD19^-$, white), non-ABC B cells ($CD19^+CD11c^-T\text{-}bet^-$, grey), or ABCs ($CD19^+CD11c^+T\text{-}bet^+$, black). Data n=6 mice per group, data compiled from two experiments, representative of three experiments. (**D**) Representative flow plot of ABCs ($CD19^+CD11c^+T\text{-}bet^+$) in the spleen gated for YFP (γHV68.H2bYFP) and IFNγ with mean ± SEM. Dot plot of the proportion of uninfected (YFP^-) and infected (YFP^+) ABCs in the spleen that express IFNγ. (**B, D**) Data presented as mean ± SEM, analyzed by Mann-Whitney test. Each data point represents an individual mouse. P-values indicated as asterixis as follows: ****$p<0.0001$.

723 **Figure 4**

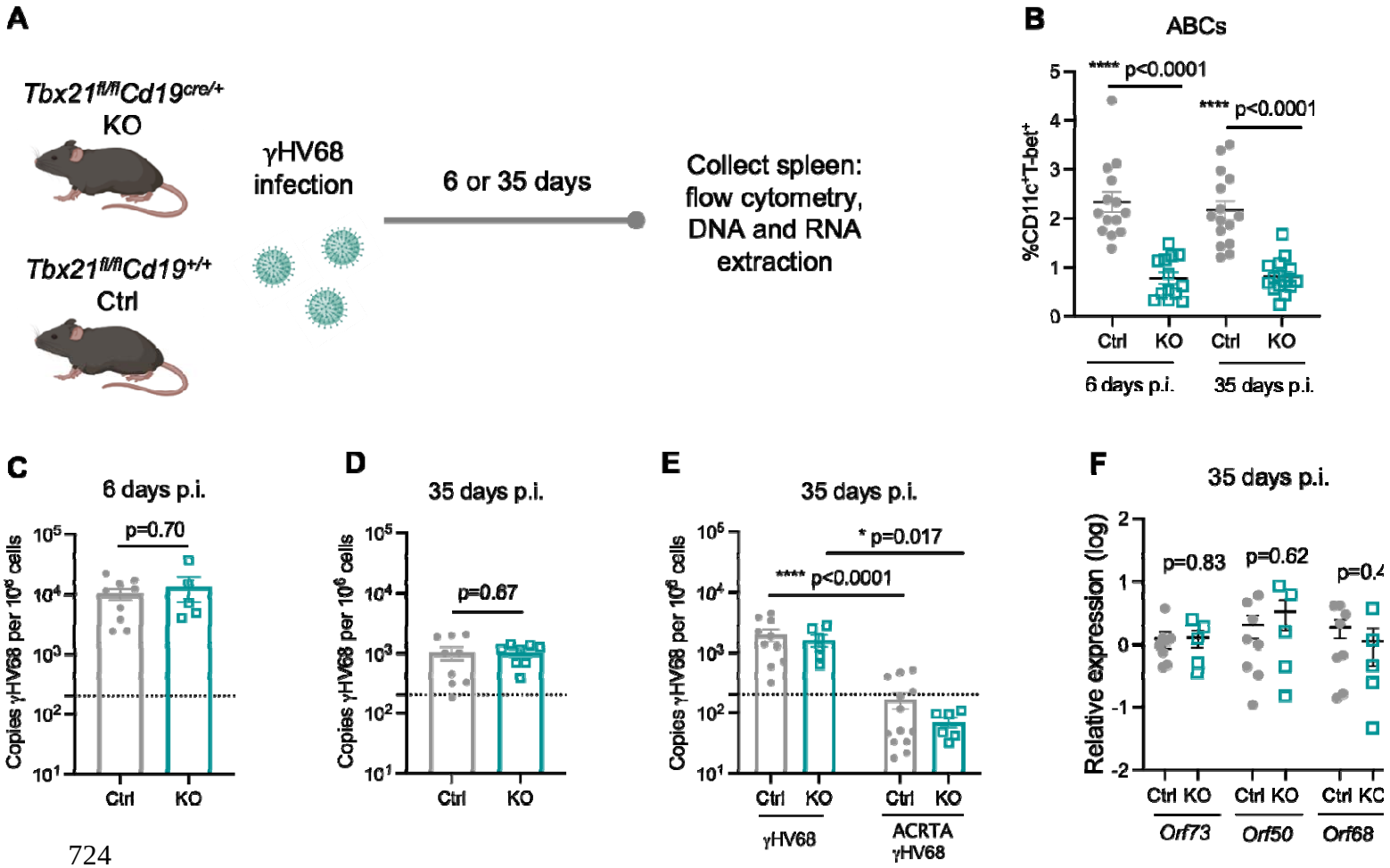

724
725

726 **Figure 4 ABCs are not required for controlling lytic infection and achieving latency**

727 *Tbx21*$^{fl/fl}$*Cd19*$^{+/+}$ (Ctrl, filled grey circles) and *Tbx21*$^{fl/fl}$*Cd19*$^{cre/+}$ (KO, open blue squares) mice
728 were infected i.p. with γHV68 or ACRTA-γHV68. 6 or 35 days p.i., spleens collected and
729 processed for RNA extraction, DNA extraction, and flow cytometry. (**A**) Experimental scheme
730 for data shown in panels B, C, D, and F. (B) Proportion of ABCs (CD11c^{+}T-bet^{+}) of mature B cells
731 (CD19^{+}IgD^{-}) in the spleen in Ctrl and KO mice 6 and 35 days post-γHV68 infection. (**C-D**) Splenic
732 γHV68 viral load (copies *Orf50* per million cells) in Ctrl (filled circles) and KO (open squares)
733 mice as determined by qPCR day 6 and 35 p.i., with limit of detection indicated by dotted line.
734 (**E**) Splenic γHV68 viral load (copies *Orf50* per million cells) in Ctrl and KO mice infected with
735 γHV68 or ACRTA-γHV68 35 days p.i.. (**F**) Relative expression in the spleen of *Orf73*, *Orf50*, and
736 *Orf68* in Ctrl and KO mice at day 35 p.i.. Each data point represents an individual mouse. Data
737 presented as mean ± SEM, analyzed by Mann-Whitney test (**B-D, F**) or one-way ANOVA (**E**).
738

739 **Figure 5**

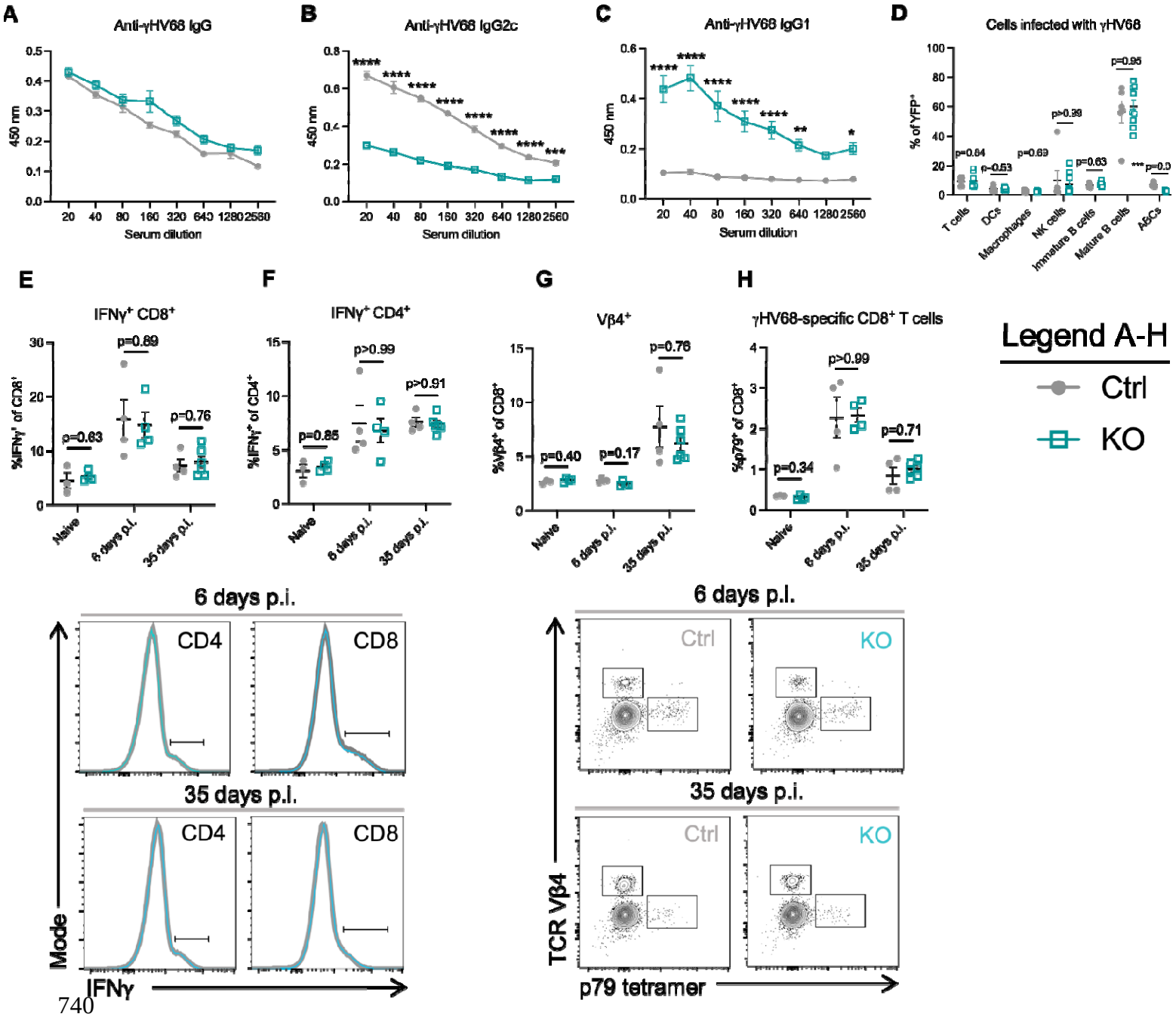

740
741

742 **Figure 5 Mice without ABCs display a dysregulated anti-γHV68 antibody response, though no**
743 **alterations to the cell populations infected with γHV68 or γHV68-responding T cells,**
744 **compared to mice with ABCs**
745
746 (**A-C**) *Tbx21*$^{fl/fl}$*Cd19*$^{+/+}$ (Ctrl, filled grey circles) and *Tbx21*$^{fl/fl}$*Cd19*$^{cre/+}$ (KO, open blue squares)
747 mice were infected i.p. with γHV68 for 6 or 35 days. N=5 per group, representative of 2
748 experiments. (**D**) Ctrl and KO mice were infected i.p. with γHV68.H2bYFP for 8 days. N=6-8 per
749 group, data compiled from 2 experiments. (**E-H**) Ctrl and KO mice were infected i.p. with γHV68
750 for 6 or 35 days, at which point spleens were collected for flow cytometry. Representative of 2
751 experiments. Each data point represents an individual mouse. Data presented as mean ± SEM.
752 Analyzed by two-way ANOVA (**A-C**) or Mann-Whitney test (**D-H**). P-values indicated as asterixis
753 as follows: ****p<0.0001, *** p<0.001, ** p<0.01, * p<0.05.
754

755 **Figure 6**

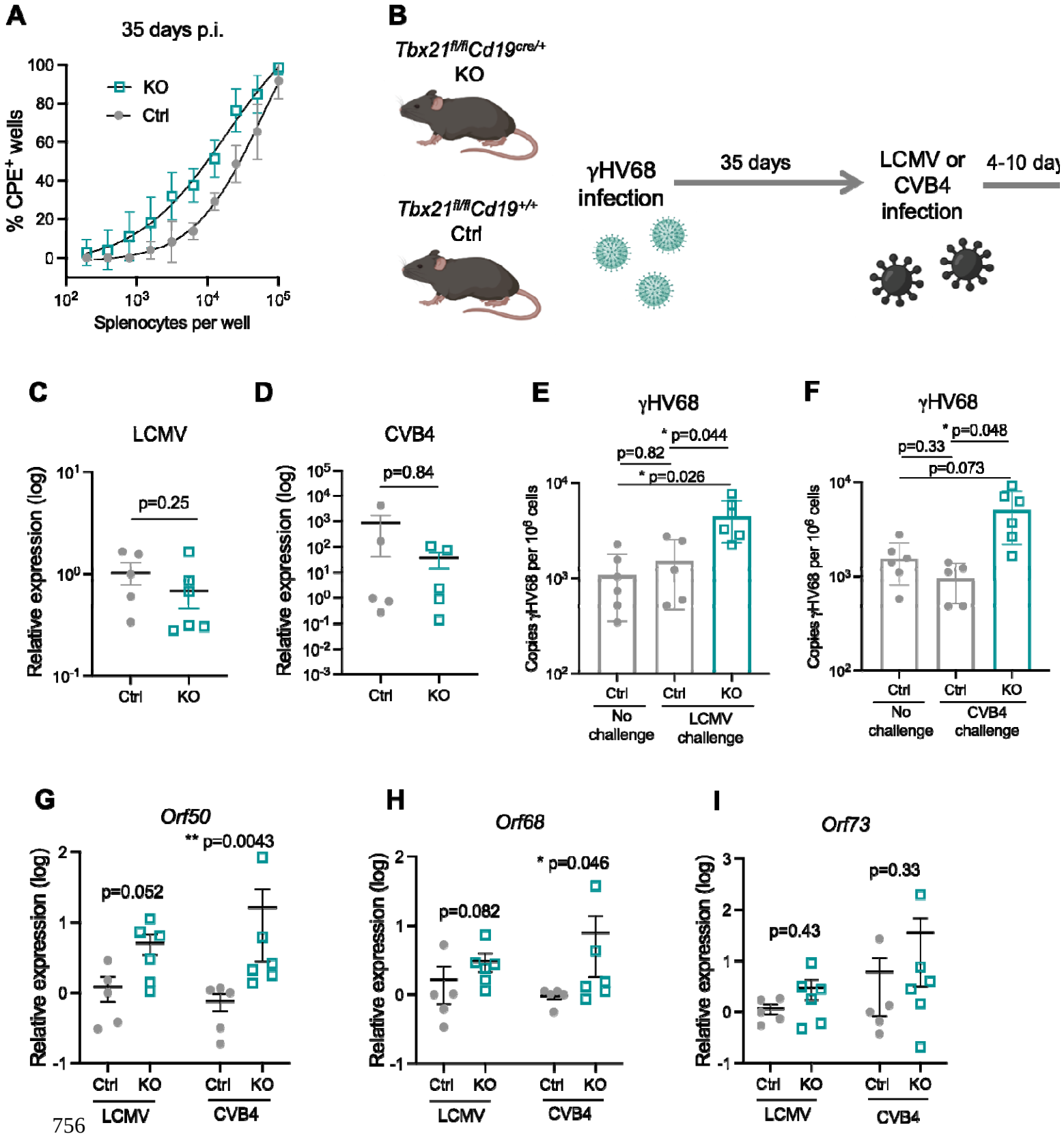

756

Figure 6 ABC knockout mice are more susceptible to reactivation

(**A**) *Tbx21*$^{fl/fl}$*Cd19*$^{+/+}$ (Ctrl, filled grey circles) and *Tbx21*$^{fl/fl}$*Cd19*$^{cre/+}$ (KO, open blue squares) mice were infected i.p. with γHV68. 35 days p.i., spleens were collected and processed for reactivation assay. N=6 mice per group, data compiled from two independent experiments. (**B**) Experimental scheme for data shown in panels C-I. Ctrl and KO mice were infected i.p. with γHV68 for 35 days and then challenged with either LCMV (Armstrong) or CVB4 for 10 to 4 days, respectively. **(C-I)** Spleens collected, processed, and DNA and RNA was extracted from total splenocytes following RBC lysis. (**C, D**) Relative expression of LCMV (**C**) and CVB4 (**D**) between Ctrl and KO mice measured by RT-qPCR. (**E, F**) Copies of γHV68 detected by qPCR in the spleen per million cells following challenge with LCMV or CVB4. (**G-I**) Relative expression in the spleen of *Orf73*, *Orf50*, and *Orf68* in Ctrl and KO mice. Each data point represents an individual mouse. Data presented as mean ± SEM, analyzed by Mann-Whitney test (**C-D, G-I**) or one-way ANOVA (**E, F**). P-values indicated as asterixis as follows: ** $p<0.01$, * $p<0.05$.